Journal of Great Lakes Research 42 (2016) 775–788

Contents lists available at ScienceDirect

Journal of Great Lakes Research

journal homepage: www.elsevier.com/locate/jglr

Internal loading of phosphorus in western Lake Erie

Gerald Matisoff [a,*], Eliza M. Kaltenberg [a], Rebecca L. Steely [a], Stephanie K. Hummel [a], Jinyu Seo [a], Kenneth J. Gibbons [b], Thomas B. Bridgeman [b], Youngwoo Seo [c], Mohsen Behbahani [c], William F. James [d], Laura T. Johnson [e], Phuong Doan [f], Maria Dittrich [f], Mary Anne Evans [g], Justin D. Chaffin [h]

[a] Department of Earth, Environmental, and Planetary Sciences, Case Western Reserve University, 10900 Euclid Avenue, Cleveland, OH 44106-7216, USA
[b] Department of Environmental Sciences, University of Toledo, Lake Erie Center, 6200 Bayshore Rd., Oregon, OH 34616, USA
[c] Department of Civil Engineering, Chemical and Environmental Engineering, School of Green Chemistry, University of Toledo, 2801 W. Bancroft St. Toledo, OH 43606, USA
[d] Department of Biology, Sustainability Sciences Institute, University of Wisconsin–Stout, Department of Biology, 123E Jarvis Hall, Menomonie, WI 54751, USA
[e] National Center for Water Quality Research, Heidelberg University, 310 E Market St., Tiffin, OH 44883, USA
[f] Department of Physical and Environmental Sciences, University of Toronto Scarborough, 1265 Military Trail, Toronto, Ontario, M1C 1A4, Canada
[g] U.S. Geological Survey, Great Lakes Science Center, 1451 Green Rd., Ann Arbor, MI 48105, USA
[h] The Ohio State University, Franz Theodore Stone Laboratory Ohio Sea Grant, P.O. Box 119, 878 Bayview Ave., Put-in-Bay, OH 43456, USA

ARTICLE INFO

Article history:
Received 3 August 2015
Accepted 7 April 2016
Available online 2 July 2016

Communicated by Noel Urban

Index words:
Lake Erie
Phosphorus
Internal loading
Western Basin
Sediments
Phosphorus flux

ABSTRACT

This study applied eight techniques to obtain estimates of the diffusive flux of phosphorus (P) from bottom sediments throughout the western basin of Lake Erie. The flux was quantified from both aerobic and anaerobic incubations of whole cores; by monitoring the water encapsulated in bottom chambers; from pore water concentration profiles measured with a phosphate microelectrode, a diffusive equilibrium in thin films (DET) hydrogel, and expressed pore waters; and from mass balance and biogeochemical diagenetic models. Fluxes under aerobic conditions at summertime temperatures averaged 1.35 mg P/m^2/day and displayed spatial variability on scales as small as a centimeter. Using two different temperature correction factors, the flux was adjusted to mean annual temperature yielding average annual fluxes of 0.43–0.91 mg P/m^2/day and a western basin-wide total of 378–808 Mg P/year as the diffusive flux from sediments. This is 3–7% of the 11,000 Mg P/year International Joint Commission (IJC) target load for phosphorus delivery to Lake Erie from external sources. Using these average aerobic fluxes, the sediment contributes 3.0–6.3 μg P/L as a background internal contribution that represents 20–42% of the IJC Target Concentration of 15 μg P/L for the western basin. The implication is that this internal diffusive recycling of P is unlikely to trigger cyanobacterial blooms by itself but is sufficiently large to cause blooms when combined with external loads. This background flux may be also responsible for delayed response of the lake to any decrease in the external loading.

Introduction

During the 1960s, Lake Erie experienced huge algal blooms, low-oxygen waters, and fish kills reflecting the effects of significant eutrophication. Research and predictions of empirical and computer ecosystem models (e.g., Charlton, 1980; Di Toro and Connolly, 1980; Schelske and Stoermer, 1971; Vollenweider, 1976) identified phosphorus (P) control as the best means of controlling eutrophication. Target levels for P loading were determined by binational collaborative programs that led to the implementation of the Great Lakes Water Quality Agreement (IJC, 1978) with a target total phosphorus (TP) loading to Lake Erie of 11,000 metric tons per year (Mg/year) and the IJC recommended programs that would achieve those loads. DePinto et al. (1986) provide a retrospective of the 1970s Great Lakes phosphorus load reduction programs. In response to those load reduction programs, phosphorus loadings declined steadily beginning in the 1970s from over 25,000 Mg/year to a 1981–2011 average of 9491 Mg/year (Baker et al., 2014). Following the initial decline in loadings phytoplankton biomass and frequency of cyanobacterial blooms decreased (Makarewicz, 1993), and oxygen depletion rates declined (Bertram, 1993). However, since about the mid-1990s, Lake Erie has experienced a number of water quality and ecosystem changes (Matisoff and Ciborowski, 2005). For example, although TP loadings have remained at or below the target loading of 11,000 Mg/year (except during wet years characterized by marked flood pulses), the extent of harmful (*Microcystis*) and nuisance (*Cladophora*) algal blooms has increased (Conroy et al., 2005a, 2005b; Michalak et al., 2013). In addition, episodic anoxia may be increasing in the bottom waters in the Central Basin (Rockwell and Warren, 2003), although there is no evidence of increased anoxia in the relatively shallow Western Basin.

There are a number of potential explanations for these ecosystem and water quality changes, including (1) increased internal loading of P possibly mediated by dreissenid mussels (Conroy et al., 2005a,

* Corresponding author. Tel.: +1 216 368 3677.
E-mail address: gerald.matisoff@case.edu (G. Matisoff).

http://dx.doi.org/10.1016/j.jglr.2016.04.004
0380-1330/

2005b), (2) underestimation of some P inputs such as from urban storm water, (3) changes in the ecosystem that have led to altered nutrient uptake mechanisms and nutrient balances in the lake, (4) increases in bioavailable P loading despite relatively constant loadings of TP (Baker et al., 2014), and (5) weather/climate induced changes that affect lake levels, the timing of nutrient pulses, and water temperatures and wind events that affect sediment resuspension and transport and nutrient release (Ohio EPA, 2010).

Seasonal variations in external nutrient loading, temperature, and internal nutrient processing may also play a role in the formation of algal blooms. Stumpf et al. (2012) and Obenour et al. (2014) showed that the biomass of summer/fall cyanobacteria in Lake Erie is directly related to spring time total P loading from the Maumee River, leading to the question of how P is recycled and retained in the western basin beyond its average water residence time. The seasonal variation in P flux could also have consequences for the lake ecology. Michalak et al. (2013) found similar causes in their analysis of the large 2011 *Microcystis* bloom and concluded that similar blooms were likely to occur in the future unless changes in agricultural loading sources and climate stressors are made. The drought in the spring of 2012 was followed by a much reduced bloom in the summer of 2012, suggesting that the effect of reducing external loading is almost immediate. However, if external loading was the only factor, there should have been almost no bloom in 2012, but the 2012 bloom, albeit smaller, was likely supported significantly by the internal load. These observations suggest that uncertainties surrounding the relative influence of the five potential explanations indicate that a better understanding of the nutrient dynamics in the western basin of Lake Erie is required in order to establish more accurate P management plans and loading targets, to forecast future water quality, and to better target remedial actions and best management practices. In particular, one of the poorly known components of the nutrient dynamics is the amount of P that is recycled to the water column by internal loading. Not only does this unknown loading create uncertainty in the determination of the total quantity of P delivered to the lake, but it also creates uncertainty in estimating the lag time between reductions in tributary loading and the time frame over which improvements in lake water quality are to be expected.

Regenerated sedimentary P is highly mobile and migrates upward to the sediment surface where it is partially retained on iron and manganese oxyhydroxides under aerobic conditions (Søndergaard et al., 2003) and partially fluxes into the water column. Under anaerobic conditions in the overlying water the oxyhydroxides are reduced and dissolve, releasing their sorbed P (Boström et al., 1998; Mortimer, 1941), a process that is enhanced in sediments with a low Al/Fe ratio (Loh et al., 2013). Fluxes under anaerobic conditions are significantly higher than those under aerobic conditions (North et al., 2015), and oxygenation of the water column, such as during fall turnover, forms ferric oxyhydroxides which scavenge phosphate and return it to the sediment (Gunnars and Blomqvist, 1997; Hoffman et al., 2013). Recently, Orihel et al. (2015) have suggested that polymixis can release P from iron poor sediments lowering nitrogen to phosphorus ratios (N:P) and stimulating cyanobacterial blooms, a process they term the "nutrient pump." However, in western Lake Erie *Microcystis* blooms are of concern, and they require higher N and higher N:P ratios than N-fixers (Reynolds, 2006). Blooms in western Lake Erie tend to occur when the total nitrogen (TN) to TP ratio is 25–100 (molar ratio) (Chaffin et al., 2013). Oxygen isotopes of dissolved phosphate have been used to identify potential sources for phosphate in the water column, and Elsbury et al. (2009) suggested that one source in Lake Erie may be the release of phosphate from sediments during anaerobic events.

Western Lake Erie is relatively shallow, averaging 7.3 m mean depth, and consequently the water column is regularly mixed and oxygenated, and bottom sediment is regularly resuspended. Although there is some P associated with the sediment particles, the particles do not remain in suspension very long. Under these aerobic conditions, little P would be expected to be released to the water column in the manner described by the Orihel et al. (2015) nutrient pump model, so that resuspension provides only a minor contribution of P to the water column. Conversely, the degradation of organic matter in anaerobic sediment would be expected to release dissolved, highly bioavailable P into the sediment pore waters where it will diffuse out of the sediment and into the water column, although as noted above some of this regenerated P will be retained in aerobic surface sediment. Here we refer to this diffusive flux of P from the sediment to the water as internal loading, and although there may be an additional, small internal loading contribution from resuspended sediment and a small removal of P by sediment deposition we do not consider those processes here.

There are a number of different techniques that have been employed to quantify this internal loading of P. For example, using biogeochemical modeling, Canavan et al. (2006) found that ~56% of the TP deposited on the sediment of Haringvliet Lake (the Netherlands) was returned to the overlying water through diffusion and bioirrigation (the pumping of pore water by benthic macroinvertebrates through their burrows). Nürnberg et al. (2013) using hypolimnion TP concentration changes and Loh et al. (2013) using core incubations estimated the internal P loading in Lake Simcoe (Ontario) to be 45 to 89% of the external load. James (2012) incubated intact sediment cores from Lake of the Woods (Minnesota) under both aerobic and anaerobic conditions and found that the diffusive P flux ranged from 8.3 to 12.5 mg P/m^2/day under anaerobic conditions and from 0.2 to 0.6 mg P/m^2/day under aerobic conditions. He concluded that the diffusive flux can represent an important contribution to the P budget of those lakes. The benthic P flux as a function of bottom water oxygen concentrations has also been measured using *in situ* bottom chambers (Noffke et al., 2012). Together, these studies build a strong case for the importance of internal P loading to a variety of lake systems. However, the comparability of the various measurement methods remains unclear as each method is applied at a different scale and involves trade-offs between precision, control, and removal from natural conditions. In addition, these methods do not measure all the same processes involved in the internal loading of P in the lake. For example, core incubations and bottom chambers do not completely eliminate phytoplankton or microbial P uptake during incubation nor do they include resuspension or deposition fluxes, so those methods effectively measure a net diffusive P flux. Conversely, methods that calculate fluxes from pore water concentration gradients calculate a gross diffusive P release rate because they do not account for any biological, mineralogical, resuspension, or deposition processes at the sediment surface on in the water column. There is not yet a scientific consensus on the most accurate method to measure the diffusive P flux, and furthermore, contrasting the results from various methods (for example, aerobic vs. anaerobic conditions) can lead to important information on system response to varying natural conditions.

The purpose of this paper is to quantify and compare estimates of the internal loading of P to the water column in the western basin of Lake Erie. Three general approaches are used to estimate the internal P loading to the water column. One approach is to quantify directly the net diffusive flux of P that is released from the sediment to the overlying water. This approach includes both aerobic and anaerobic incubations of whole cores (James, 2012) and the monitoring of the water encapsulated in chambers placed on the lake floor (Tenberg et al., 2004). Whole core incubations under anaerobic conditions are of interest because the shallow water of the western basin can occasionally stratify for time periods of up to 5 days and the bottom waters can go anaerobic (Bridgeman et al., 2006).

A second approach to estimate the internal P loading to the water column is to measure the phosphate concentrations in the pore waters near the sediment–water interface and calculate the Fickian diffusional flux from the sediment to the overlying water. This approach calculates the gross diffusional P flux from the sediment. The difficulty with this method is one of obtaining the concentration gradient at the sediment–water interface because pore waters expressed from centimeter-scale slices of sediment may not provide sufficient accuracy.

Flux calculations based on pore water concentration gradients are also dependent on the thickness of the benthic boundary layer, which is difficult to measure. A much higher resolution concentration profile can be obtained with a phosphate microelectrode (Ding et al., 2015; Korostynska et al., 2012; Lee et al., 2009) or a phosphate DGT or DET gel (Davison et al., 2000), and both electrodes and DET techniques are employed in this study. In addition, we estimate the flux from cm-scale expressed pore water measurements of dissolved phosphate.

The third approach to estimate the internal P loading to the water column uses mass balance and biogeochemical diagenetic models to estimate the gross diffusive phosphate flux from the sediment. These models use a variety of techniques to obtain the concentration gradient at the sediment–water interface, such as 2-layers (aerobic and anaerobic) (DiToro, 2001) or reactive, multi-component, linked sediment solids and sediment pore waters (Dittrich et al., 2009; Wang and Van Cappellen, 1996). Here we apply both a modified version of the DiToro (2001) model to estimate the P diffusive flux by a mass balance of the difference between the depositional and burial P fluxes and a biogeochemical diagenetic model (Dittrich et al., 2009) to calculate pore water concentrations and estimate phosphate fluxes.

In this study, we present estimates of the internal diffusive flux of phosphate calculated using all three approaches: (1) direct net fluxes determined by laboratory aerobic and anaerobic incubations of sediment cores and by field-deployed bottom chamber incubations; (2) Fickian calculations of gross P fluxes determined by phosphate concentrations obtained by microelectrodes, by discrete sediment pore waters, and by phosphate DETs; and (3) gross fluxes determined by a mass balance model and by a biogeochemical model. Of particular note is that we have applied different methods that are frequently employed by different researchers and in different locations in order to compare them to each other and to obtain better estimates of basin-wide P fluxes and their variability. As such, we have pooled the data sets so not all methods were conducted at all locations or even in the same year. This obviously can lead to some limitations in interpreting the data, but we have used multiple methods simultaneously at the same location to build confidence in inter-method comparisons and believe that the benefits of pooling the data sets to obtain a basin-wide perspective of the P flux from bottom sediments far outweighs the remaining limitations.

Methods

Core collection and bottom chamber placements

Intact sediment cores 6.5 cm internal diameter (ID) and 50 cm length were collected from 5 locations near the Maumee River mouth on June 24, 2013, using a gravity coring device (Aquatic Research Instruments, Hope ID) equipped with an acrylic core liner. The core liners, containing both sediment and overlying water, were immediately sealed using rubber stoppers and stored in a covered container on ice until transport to the laboratory. Similar but not exactly the same methods were used to collect the cores at the remaining sites.

On July 6, 2013, a 6.7-cm ID core was collected from the R/V Lake Guardian using a 1.5-m Benthos gravity corer. Upon retrieval, the core tube was immediately capped and secured with tape. It was stored in a vertical position in the refrigerator on the ship until transport to the lab. In the lab, the cap of the core tube was removed to allow oxygen into the overlying water so that it did not become anaerobic prior to analysis.

From June 27 through August 4, 2014 ten locations in western Lake Erie were sampled by divers using SCUBA (Fig. 1). Core tubes 6.7 cm ID and 15 cm in length were obtained for aerobic (2 cores) and anaerobic (3 cores) incubations to monitor the phosphate release from sediments, for phosphate microelectrode profiling (3 cores), and for phosphate DETs (2 cores). At 4 additional locations (91M, C40, C5, and 61), cores were collected from the R/V Lake Guardian by subsampling an Ekman 30 cm × 30 cm box corer with 6.7 cm ID cellulose acetate butyrate core tubes 15 cm in length. After collection, the cores were capped and returned to the laboratory and refrigerated with the top caps removed during storage until needed for analysis. At 7 stations (WQ2, WQ3, WQ6, 3P, NBIw, BIM, and SBI-KI), divers placed chambers on the lake bottom. One or two chambers were placed at each station about 10 m apart. These chambers were sampled periodically by divers over 1 to 4 days to monitor the oxygen and phosphate concentrations in the enclosed water. Water samples were returned to the laboratory for analysis.

Net direct flux measurements

Aerobic and anaerobic incubations

Incubations on cores from the Maumee River dredge disposal area were conducted at University of Wisconsin–Stout and on cores from the rest of the Western Basin at Case Western Reserve University and at the University of Toledo. All core incubations were processed in similar but not identical ways. The cores collected near the Maumee River dredge disposal area were processed as follows. Sediment cores were carefully drained of overlying water, and the upper 10 cm layer was transferred intact to a smaller acrylic core liner (6.5 cm ID and 20 cm height) using a core remover tool. Water collected from the western basin was filtered through a glass fiber filter (Gelman A-E; 2.0 μm nominal pore size); 300 mL was then siphoned onto the sediment contained in the small acrylic core liner without causing sediment resuspension. The sediment incubation systems were placed in a darkened environmental chamber and incubated at a constant temperature for up to 2 weeks. The incubation temperature was maintained at 20 °C to simulate average summer temperatures. The oxidation–reduction environment and the mixing of the overlying water were controlled by gently bubbling either air (aerobic) or nitrogen (anaerobic) through tubing placed just above the sediment surface. Anaerobic conditions were verified using a dissolved oxygen electrode. Water samples for soluble reactive phosphorus (SRP) were collected at 1- to 3-day intervals over the entire incubation period. Samples (10 mL) were collected from the center of each sediment incubation system using a syringe and immediately filtered through a 0.45-μm membrane syringe filter. The water volume removed from each system during sampling was replaced by addition of filtered lake water preadjusted to the proper oxidation–reduction condition. These volumes were accurately measured for determination of dilution effects. SRP was measured colorimetrically using the ascorbic acid method (American Public Health Association, 1989). Rates of SRP (expressed as P) release from the sediment (mg P/m^2/day) were calculated as the linear time rate of change in concentration in the overlying water divided by the area of the incubation core liner as given in Eq. (1):

$$F = \mathrm{d}C/\mathrm{d}t{*}V/A \quad (1)$$

where

F	is the phosphate flux (mg SRP/m^2/day),
dC/dt	is the time rate of change of the SRP concentration in the water overlying the sediment (mg SRP/L/day),
V	is the volume of water overlying the sediment (L), and
A	is surface area of the core exposed to the overlying water (m^2).

Fluxes were then converted from phosphate flux (mg SRP/m^2/day) to P flux (mg P/m^2/day) by assuming SRP is HPO_4^{2-}, and the results are reported in Table 1.

For the remaining aerobic incubations of Western Basin cores, two cores from each sampling location were incubated at 23 ± 2 °C. The majority of the water in the core tube overlying the sediment was removed and replaced four times with bottom water to a volume of 120 mL to remove buildup of P. The core was capped, the water was stirred at about

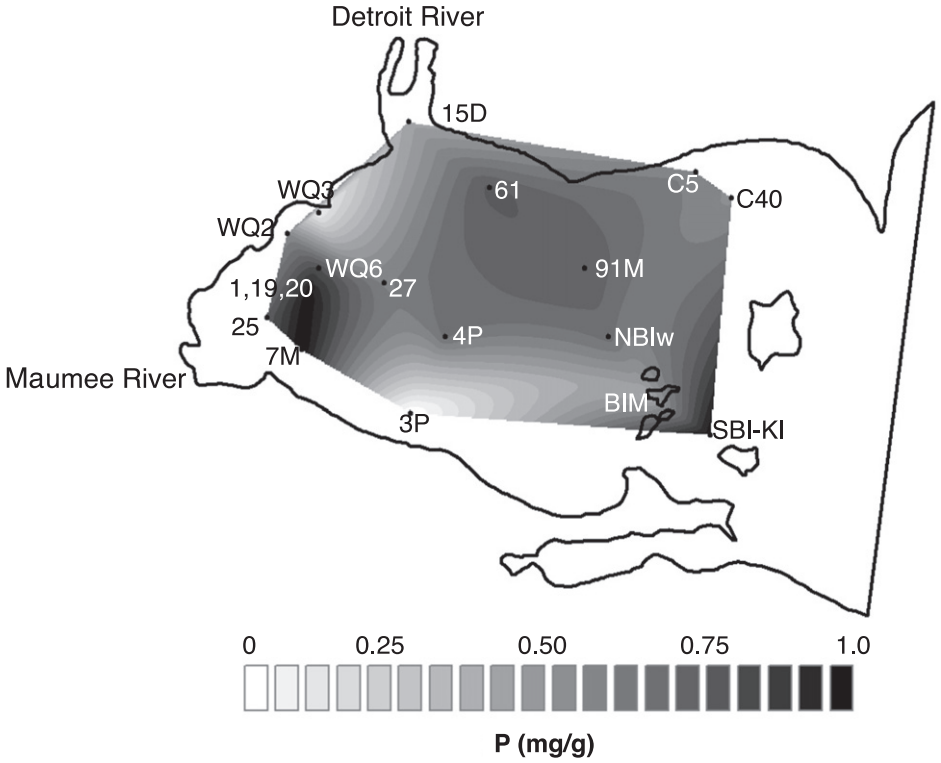

Fig. 1. Map of station locations in the western basin of Lake Erie. Shading shows the contours of the concentrations of total phosphorus in the surface sediments.

60 rpm 1 cm above the sediment, and oxygen saturation was maintained by slowly bubbling air in the overlying water. Aliquots (2.5 mL) and temperature and oxygen readings were taken at 1 h, 4 h, 6 h, 8 h, and 24 h. The water samples were filtered through a 0.45-μm nylon syringe filter and analyzed for SRP using the ascorbic acid method (Strickland and Parsons, 1972), modified for small sample volumes. To

Table 1
Sampling locations and phosphorus fluxes (as P) (mg P/m^2/day) obtained by the different techniques.

Station name	Date(s) sampled	Latitude	Longitude	Depth (m)	P (mg/g)	Incubation		Bottom Chamber	P-electrode		P-DET[a,b]	Expressed pore water	Mass balance model	Diagenetic model[c]
						Aerobic	Anaerobic		Aerobic	Anaerobic				
1[d]	6/24/2013	41.8049 N	83.2868 W	4.6	0.970	0.16, 0.34	2.41, 3.10							
19[d]	6/24/2013	41.81409 N	83.2825 W	5.8	0.905	0.26, 0.22	7.37, 4.78							
20[d]	6/24/2013	41.81437 N	83.2846 W	5.8	0.945	0.19, 0.31	6.62, 5.42							
25[d]	6/24/2013	41.7754 N	83.3438 W	5.2	0.740	0.56, 1.08	13.29, 12.88							
27[d]	6/24/2013	41.8214 N	83.1855 W	7.9	0.575	0.83, 0.38	16.73, 20.78							
91M[e]	7/06/2013	41.841 N	82.916 W	10.3		2.67	0.58					0.79	4.93	2.38
91M[f]	7/22/2014	41.841 N	82.916 W	10.3	0.726	0.87, 1.15	4.27, 1.17, 1.15				2.17, 1.72, (*1.95*, *1.87*)			
15D[f]	7/30–8/4/2014	42.033 N	83.153 W	3.0	0.416	1.48					(0.90)			
WQ3[f]	7/31–8/1/2014	41.914 N	83.274 W	5.5	0.089	0.97		0.79						
WQ2[f]	7/30–8/4/2014	41.886 N	83.316 W	3.5	0.545			0.93, 0.13			5.84, 2.32			
WQ6[f]	7/30–8/4/2014	41.841 N	83.274 W	6.5	0.783	2.16, 2.91		2.97, 2.77			(8.26), 2.39			
7M[f]	6/27–28/2014	41.733 N	83.297 W	5.5	0.982	0.71	5.00, 27.26, 3.01		1.89	1.96	1.09, 3.81			
4P[f]	6/27–28/2014	41.750 N	83.104 W	9.5	0.647	1.70	1.06, 1.55, 7.03	1.70, 1.87		0.79				
61[f]	7/22/2014	41.947 N	83.044 W	7.5	0.749	0.65, 0.96					1.75, 3.88, (*2.88*, *3.40*)			
NBIw[f]	7/14–18/2014	41.750 N	82.884 W	9.0	0.660	0.66		0.09, 0.35			5.65, 2.06			
BIM[f]	7/14–18/2014	41.670 N	82.830 W	9.0	0.385	0.47, 0.74		0.16			1.16, 0.60			
KI-SBI[f]	7/14–18/2014	41.621 N	82.747 W	8.5	0.968	0.44, 1.26		0.05, 0.22			2.44, 3.23			
C5[f]	7/22/2014	41.967 N	82.767 W	9.5	0.569	1.90, 1.16	1.18, 1.53, 0.64		0.01	2.50	1.47			
C40[f]	7/22/2014	41.933 N	82.718 W	10.5	0.527	1.05, 1.67					1.42			

[a] Values in parenthesis are from same core as aerobic incubation.
[b] Values in italics are from the same core, except that they are facing opposite directions.
[c] Dittrich et al. (2009).
[d] Ten-day incubations.
[e] One-day incubations.
[f] One-day aerobic, 4-day anaerobic incubations.

correct for volumetric changes caused by sample withdrawals, SRP concentrations (mg/L) in the core tube are converted to phosphate masses (mg) by multiplying by the water volume at the time of sampling. Phosphate mass increased linearly with time during the initial 8 h but approached an equilibrium concentration after 24 h. Thus, SRP fluxes (mg SRP/m^2/day) were calculated as the slope of the initial linear increase in phosphate mass with time (mg/day) divided by the cross sectional area of the core tube (m^2) as shown in Eq. (1). Fluxes were then converted from phosphate mass flux (mg SRP/m^2/day) to P flux (mg P/m^2/day) and reported in Table 1.

Anaerobic incubations conducted at the University of Toledo were completed on cores collected during the summer of 2014 from stations 4P, 7M, 91M, and C5. After collection, cores were stored in a 4 °C fridge without the caps in order to keep the cores aerobic until needed for incubation. Prior to incubation, the overlying water was removed and replaced with 500 mL of lake water filtered through a 0.45-μm filter (Millipore GWSC 045). Temperature was controlled by placing the cores in an incubation chamber (Percival E36HO) set at 20 °C where the cores were incubated for 4 days. The dissolved oxygen in the overlying water was maintained at 0 mg/L by gently bubbling nitrogen. Water samples (10 mL) were taken daily, filtered, and frozen for later analysis. Dissolved oxygen and temperature of the overlying water was checked to ensure that the cores were anaerobic and at the desired temperature. At the end of the incubation, the top 1 cm of the sediment was extruded and analyzed for organic content by loss on ignition (Schumacher, 2002). Water samples were analyzed for SRP in accordance to EPA method 365.2. Flux calculations were done in same manner as the other incubations as given in Eq. (1), and the results are reported in Table 1.

It has been reported that the first 2–3 days of anaerobic incubations should be excluded from flux calculations (Loh et al., 2013) because of a change in microbial electron acceptors. The longer anaerobic incubations (on cores from the Maumee River dredge disposal area) did show a change after 2 days, so the initial data in those incubations were excluded from the flux calculations. However, the data from the 4-day incubations presented here are linear over the entire 4-day incubation time indicating that all the data could be used in the calculation of phosphate fluxes.

Bottom chambers

The bottom chambers were constructed from 19 gal Sterilite® plastic containers and measured 2232 cm^2 surface area × 19 cm height. The enclosed water was recirculated through the chamber at a flow velocity of 1.5 L/min by a Dynamax DM100vv DC pump powered by a car battery. With a chamber water volume of 42.5 L this gives a water residence time of approximately 28 min. The chambers were inserted by divers using SCUBA into the bottom to a known depth demarcated by a shelf around the outside of the chamber. Bottom chambers were sampled by divers attaching syringes to a valve and withdrawing seven 60–65 mL aliquots for a total volume of ~435 mL per sample. The withdrawn sample volume was replaced by water from a loose bag filled with lake water that collapsed as water was withdrawn from the chamber. This prevented sediment pore water from being drawn into the chamber during sample withdrawal. These chambers and ambient lake water near the chambers were sampled daily by divers for times up to 4 days to monitor the oxygen and SRP concentrations in the enclosed water. Ambient lake water outside the chambers was sampled by opening an empty 500 mL bottle and allowing it to fill. Syringes and bottles were returned to the research vessel and held on ice during transportation to the laboratory. Dissolved oxygen concentration and water temperature were measured by slowly ejecting water from a syringe into a 500-mL bottle then inserting the probe of a calibrated YSI-550A into the bottle.

All water samples were analyzed for both SRP and for TP using EPA method 365.2. For SRP measurements, samples were filtered through a 0.45-μm membrane filter within 24 h of collection and analyzed. For TP measurements, samples underwent a persulfate digestion and were analyzed by molybdate blue colorimetry using a Seal AutoAnalyzer 3. Additional detailed standard operating procedures (SOPs), detection limits, and quality control protocols are given in the Quality Assurance Project Plan (QAPP) appendices developed for the Honey Creek Targeted Watershed Project posted online here: http://www.heidelberg.edu/sites/default/files/dsmith/pdf/NCWQR%20-%20HC%20TWG%20QAPP.pdf.

Phosphorus fluxes were calculated using Eq. (1). SRP concentrations (mg/L) in the bottom chamber are converted to masses (mg) by multiplying the concentrations by the volume of water (L) in the chamber at the time of sampling. SRP mass increased linearly with time, permitting SRP fluxes (mg SRP/m^2/day) to be calculated as the slope of the increase in SRP mass with time (mg/day) divided by the cross sectional area of the chamber (m^2). Fluxes were then converted from phosphate flux (mg SRP/m^2/day) to P flux (mg P/m^2/day) by assuming SRP is HPO_4^{2-}, and the results are reported in Table 1.

Fickian calculations of gross phosphorus flux

Phosphate DET (diffusive equilibrium in thin films)

Phosphate DET samplers consisted of a 4-cm × 10-cm piece of acrylamide hydrogel mounted on a 1/32″-thick impact modified acrylic (ePlastics.com) backing plate and protected from physical damage by a 0.45-μm hydrophilic polyethersulfone membrane filter (STERLITECH.com). The front face of the sampler consisted of an acrylic front plate with a 4-cm × 10-cm exposure window, and the whole assembly was held together by nylon screws. The hydrogel casting solution was prepared following the method described by Jézéquel et al. (2007), except the amount of TEMED was reduced to 25 μL. The mixture was pipetted between glass plates of a gel caster (GE Health Sciences) and allowed to set at 37 °C for about 10 min. The gels were rinsed off and soaked in deionized water (DI) with at least 3 complete water changes prior to use. The gel samplers were inserted into a sediment core tube and allowed to equilibrate with overlying and pore water overnight at 17 ± 1 °C. The cores were uncapped to keep the cores aerobic, but no active aeration through bubbling was provided. "Staining gels" consisted of 4 cm × 10 cm pieces of hydrogel soaked for 2–2.5 h in color developing reagent, prepared according to the ascorbic acid method for colorimetric SRP determination (American Public Health Association, 1989). Upon retrieval, the DET samplers were briefly rinsed with DI and then disassembled to recover the gels ("sample gels"). The sample gels were placed on a glass sheet, overlaid with staining gels, then covered with a transparency sheet and taped around the edges to minimize evaporation. The whole assembly was scanned after 21 min using a conventional flatbed scanner. Gel calibration standards were prepared using 3 cm × 3 cm pieces of hydrogel equilibrated overnight in standard solutions and subsequently treated the same way as the sample gels. The images were processed and calibrated using ImageJ 1.48v and Microsoft Excel to obtain depth profiles of phosphate concentration. Since the sediment–water interface is not perfectly flat, the profiles could not be horizontally averaged. Instead, 9 vertical profiles were obtained from each image by analyzing narrow rectangular sections (slices) totaling 18% of the picture width. SRP flux through the sediment–water interface was calculated assuming Fickian diffusion using Eq. (2) (Boudreau, 1996):

$$F = -\frac{\varphi \cdot D_0}{\theta^2}\,\frac{\partial C}{\partial z} \tag{2}$$

where

F is the SRP flux (mg SRP/m^2/day),
φ is the sediment porosity (dimensionless),
D_0 is the solute diffusion coefficient for di-hydrogen phosphate at 18 °C (7.15×10^{-6} cm^2/s; Li and Gregory, 1974; 6.18×10^{-5} m^2/day),
θ is the sediment tortuosity (dimensionless),

C is the solute concentration (mg/L) phosphate, and
z is depth (m).

Tortuosity was calculated using the equation (Boudreau, 1996):

$$\theta^2 = 1 - \ln(\varphi^2) \quad (3)$$

The SRP concentration gradient at the sediment surface, $\frac{\partial C}{\partial z}|_{z=0}$, is the slope of the line fitted to the topmost linear part of the concentration vs. depth data (typically 4 mm or less). The value of the gradient for each sample was calculated as the mean of the slopes obtained from the 9 rectangular slices. Fluxes were then converted from phosphate flux (mg SRP/m^2/day) to P flux (mg P/m^2/day) by assuming SRP is HPO_4^{2-} and the results are reported in Table 1.

Phosphate microelectrode

A phosphate microelectrode is not yet commercially available, and therefore its fabrication was necessary. A phosphate-sensitive potentiometric microelectrode is constructed from cobalt wire oxidized to cobalt oxide. Phosphate ions in solution react with the cobalt oxide and a phosphate precipitate will be formed at the electrode surface depending on the pH (Eqs. (4)–(6)):

$$3CoO + 2H_2PO_4^- + 2H^+ \leftrightarrow Co_3(PO_4)_2 + 3H_2O \quad \text{at pH 4.0} \quad (4)$$

$$3CoO + 2HPO_4^{2-} + H_2O \leftrightarrow Co_3(PO_4)_2 + 4OH^- \quad \text{at pH 8.0} \quad (5)$$

$$3CoO + 2PO_4^{3-} + 3H_2O \leftrightarrow Co_3(PO_4)_2 + 6OH^- \quad \text{at pH 11.0} \quad (6)$$

The potential changes due to these reactions can be converted to phosphate concentrations (Ding et al., 2015; Xiao et al., 1995).

A section of cobalt wire (0.1 mm diameter, 99.99% pure, Sigma Aldrich) was cut and inserted into a pulled glass micropipette (OD: 1.2 mm, ID: 0.69 mm, 15 cm length; Sutter Instrument Co.). The micropipette was then melted using a heating filament (Sutter Instrument Co.) to seal the cobalt wire in the glass micropipette. After that, the microelectrode tip was beveled using a diamond abrasive plate (Sutter Instrument Co.) to a 45° angle to expose the cobalt surface. Finally, the microelectrode was connected to a copper wire using bismuth alloy (44.7% bismuth, 22.6% lead, 19.1% indium, 8.3% tin, and 5.3% cadmium) (Lee et al., 2009). The microelectrode is then immersed in DI water to form a cobalt oxide (CoO) layer on the tip of the surface. To measure sensor responses to phosphate ion concentrations, the potential between the fabricated microelectrode and the reference microelectrode (Ag/AgCl reference mini-electrode, MI-401; Microelectrodes Inc.) was monitored using a millivolt meter (Model 250, Denver Instrument). After the potential stabilized, the microelectrode was removed from the DI water and immersed into a potassium phosphate (KH_2PO_4, 10^{-4} M) solution at pH 7 until obtaining a new stable potential. After finishing pretreatment, the microelectrode was calibrated using phosphate standard solutions with concentrations ranging from 10^{-1} M to 10^{-8} M (KH_2PO_4). If stable signals were not observed from the prepared microelectrode, a new microelectrode was prepared.

Phosphorus fluxes under both aerobic and anaerobic conditions were calculated assuming Fickian transport across a boundary layer. The calculation is based on an assumption that the flux (J_{f,X_s}) of phosphate diffusing from the sediment to the surface of the sediment is equal to the phosphate flux (J_{W,X_s}) across the surface bulk solution (Lee and Bishop, 2009; Lewandowski and Beyenal, 2014):

$$J_{f,X_s} = D_f\left(\frac{dC}{dx}\right)_{f,X_s} = D_w\left(\frac{dC}{dx}\right)_{w,X_s} = J_{w,X_s} \quad (7)$$

where

J_{fXs} is the flux of phosphate from the sediment to the surface,
D_f is the phosphate diffusivity in sediment,
$(dC/dx)_{fXs}$ is the concentration gradient in the boundary layer below the sediment surface,
D_w is the phosphate diffusivity in the bulk water (7.5×10^{-6} cm^2/s at 20 °C; Krom and Berner, 1980), and
$(dC/dx)_{wXs}$ is the concentration gradient in the boundary layer above the sediment surface.

The solution to this is given by Lee and Bishop (2009) as follows:
In bulk solution,

$$\left(\frac{dC}{dx}\right)_{w,X_s} = B(C_s - C_b) \quad (8)$$

$$-B(x - x_s) = \ln\left(1 - \frac{C - C_s}{C_s - C_b}\right) \quad (9)$$

where

x_s is the sediment surface = 0 cm,
x is local depth (cm),
C_s is the SRP concentration at the surface (mg/L),
C is the local SRP concentration (mg/L), and
C_b is the stable SRP concentration in bulk water, and
B is a constant.

In this work fluxes were calculated from the measured SRP concentration at the sediment surface and in the bulk water using Eq. (7). First the coefficient "B" was obtained using Eq. (9). That value was substituted into Eq. (8) to obtain the concentration gradient, and then the value for the gradient was substituted into Eq. (7) and multiplied by D_w to obtain the flux. Fluxes were then converted from phosphate flux (mg SRP/m^2/day) to P flux (mg P/m^2/day) by assuming SRP is HPO_4^{2-} and the results are reported in Table 1.

Expressed pore water samples

Expressed pore waters were obtained from only one core at Station 91M in 2013. The core was extruded in 2 cm sections and the sediment placed in a Reeburgh-type squeezer in a nitrogen-filled glove box. Nitrogen gas pressure pushed down onto a latex sheet, which covered the sediment and forced the pore water through a 0.22-μm membrane filter and the water collected into a 4-oz polypropylene bottle. Soluble reactive phosphorus was determined within 24 h on a 5-mL aliquot using the ascorbic acid method (Strickland and Parsons, 1972), modified for small sample volumes. The phosphate flux was calculated using the concentration gradient obtained from the top 2 samples and assuming Fickian diffusion using Eq. (2). Fluxes were then converted from phosphate flux (mg SRP/m^2/day) to P flux (mg P/m^2/day) by assuming SRP is HPO_4^{2-} and the results are reported in Table 1. The pore water and bulk sediment chemical concentrations, including the phosphate data, obtained from this core were also used in the mass balance model and in the biogeochemical model.

Modeling techniques for gross phosphorus flux

Mass balance model

The mass balance model was based on DiToro (2001) where the sediment column is represented as two layers each characterized by specific organic matter diagenetic mineralization. However, in the method employed here the diagenetic production of P, $J_{p,d}$, is calculated simply as the difference between the depositional flux of organic P and the burial flux of organic *P*. The flux of P from the sediment to the overlying water, $J_{p,s\text{-}w}$, is then calculated by subtracting the burial flux of P from the diagenetic production of P. This simplified model assumes a steady-state balance between mineral precipitation and/or sorption of phosphate onto sediment particles such as iron or manganese oxides

or calcite and by the dissolution of those solids upon burial. The P flux from the sediment is given by the mass balance in Eq. (10):

$$J_{p,s-w} = J_{p,d} - \omega[PO_4] \quad (10)$$

where

$J_{p,s-w}$ is the flux of P from the sediment to the overlying water (mg P/m^2/day),
$J_{p,d}$ the diagenetic production of dissolved P (mg P/m^2/day), calculated as the difference between the organic P concentration at the top of the core (mg P/g sed) minus the organic *P* concentration at the bottom of the core (mg P/g sed) times ω, the mass sedimentation rate (g sed/m^2/day),
ω is the mass sedimentation rate calculated from the depth of the ^{137}Cs maximum in the core (=0.178 g/cm^2/year at Station 91M), and
$[PO_4]$ is the dissolved phosphate concentration (mg SRP/L) that is buried at depth in the core, converted to P concentration (mg P/g).

Fluxes (mg P/m^2/day) were then reported in Table 1.

Diagenetic model

A 1-dimensional Aquasim non-steady-state transport reactive model for sediment diagenesis of solid and dissolved substances was implemented in a new sediment compartment available in version 2.1e of the computer program Aquasim (Dittrich et al., 2009; Reichert, 1994), designed for simulation and data analysis of aquatic systems. This program solves the partial differential Eqs. (11) and (12) by firstly discretizing their spatial derivatives and then numerically integrating the resulting system of ordinary differential equations in time with the DASSL implementation (Petzold, 1983). The identifiability analysis was performed with the IDENT package (http://www.aquasim.eawag.ch).

Briefly, the two following differential equations are used to describe the vertical profiles of biogeochemically reactive solids and solutes:

$$\frac{\partial(\theta S_i)}{\partial t} = \frac{\partial}{\partial z}\left(D_B \frac{\partial(\theta S_i)}{\partial z} + \theta D_{S_i} \frac{\partial S_i}{\partial z}\right) + r_{S_i} - a_{\text{bioirrig}} * \theta * \left(S_i - S_i^{SWI}\right) \quad (11)$$

$$\frac{\partial(X_i)}{\partial t} = -\frac{\partial(v_{sed} X_i)}{\partial z} + \frac{\partial}{\partial z}\left(D_{B,X_i} \frac{\partial X_i}{\partial z}\right) + r_{X_i} \quad (12)$$

where

X_i is the concentration of particulate substance i in the sediments (mass per total sediment volume; kg/m^3),
S_i is the concentration of dissolved substance i in the sediment pore water (mass per pore water volume; kg/m^3),
S_i^{SWI} is the concentration of dissolved substance i in the water column at the sediment–water interface (kg/m^3),
t is time (days),
z (m) is depth within the sediment ($z_{SWI} = 0$ at the sediment surface, positive downward),
D_{Si} is the molecular diffusion coefficient of dissolved substance i (m^2/day),
v_{sed} is the velocity of movement of the solid phase of the sediment relative to a coordinate system with an origin at the sediment surface (m/day),
D_B is the bioturbation coefficient (m^2/day),
$D_{B,Xi}$ is the effective diffusion coefficient of particulate substance *i* (m^2/day),
r_{Si} is the total transformation rate of dissolved substance *i* (mass per total sediment volume and time; mg/L/day),
r_{Xi} is the total transformation rate of particulate substance i (mass per total sediment volume and time; mg/L/day), and.
θ is the porosity of the sediments.

Once the vertical concentration profile of phosphate was obtained, the phosphate concentration gradient at the sediment–water interface was used to calculate the phosphate flux according to Eq. (2). Fluxes were then converted from phosphate flux (mg SRP/m^2/day) to P flux (mg P/m^2/day) by assuming SRP is HPO_4^{2-} and the results are reported in Table 1.

Statistical analyses

Correlation between fluxes measured by different methods and between fluxes and sediment P concentration was assessed by Pearson's product–moment correlation coefficient, *r*. One-way ANOVA was used to test the differences in flux estimates obtained (1) by different methods used in this study and (2) from different sediment sampling stations (spatial variability). A one-sample *t*-test was used to calculate the basin-wide mean SRP flux under aerobic and anaerobic conditions. The data were tested for normality and homoscedasticity prior to any further parametric tests. When needed, a Box–Cox procedure was used to transform the data. All statistical analyses were conducted using Minitab 16. Statistical significance was assessed at the $\alpha = 0.05$ level.

Results

The TP concentrations in surface sediment samples from eighteen locations are mapped in Fig. 1 where contours of TP concentration were calculated using the "natural neighbor" option in ArcGIS, which interpolates a raster surface from discrete points. The data indicate that the sediments have TP concentrations that range from a low of about 0.1 mg TP/g along the western, Michigan shoreline to almost as high as 1 mg TP/g near the Maumee Bay. This distribution suggests that much of the P in the sediments reflects the source of the P to the western basin: the low concentrations are near the Detroit River discharge and the high concentrations are near the Maumee River discharge (Ohio EPA, 2010).

Estimates of the flux of P from the sediments obtained by aerobic and anaerobic incubations, *in situ* bottom chambers, phosphate DET gels, phosphate microelectrodes, expressed pore waters, and from the diagenetic and mass balance models are summarized in Table 1. At most locations fluxes were measured in duplicate or triplicate. Incubation results, shown in Fig. 2 show that concentrations of SRP increased linearly with time for times ranging from 8 h (aerobic incubations) to 4 to 10 days (anaerobic incubations). Phosphorus fluxes ranged from a low of 0.16 mg P/m^2/day at Station 1 under aerobic conditions to a high of 27.26 mg P/m^2/day at 7M under anaerobic conditions. There was no statistical difference between aerobic incubation fluxes between cores from 2013 and 2014 collections ($\alpha = 0.05$, ANOVA, Tukey test), so the data from 2013 were combined with the data from 2014. The fluxes did not appear to be correlated with TP concentrations in the surface sediment ($r = -0.282$, $p = 0.272$), although there is a correlation between TP and anaerobic incubation P fluxes at 30 °C (but not at 20 °C, data not shown).

It has been suggested that under anaerobic conditions P release rates increase after a couple of days, possibly because of sulfate reduction, so that the data from the first couple of days need to be excluded (Loh et al., 2013). There may be some evidence for this in the longer incubation data, so in those cases, the data from the first day or so were excluded from the calculation of the release rate for both aerobic and anaerobic incubation conditions (Fig. 2). However, the 4-day anaerobic incubations show no evidence for this, so all data were used to determine the release rate (Fig. 2). There was no statistically significant difference in the average P flux obtained from the 4-day and the 10-day anaerobic incubations ($p = 0.25$, 2-sample *t*-test), although these data were obtained at different locations. The average anaerobic flux was 4.57 ± 4.87 mg P/m^2/day in the 4-day incubations vs. 9.34 ± 6.48 mg P/m^2/day in the 10-day

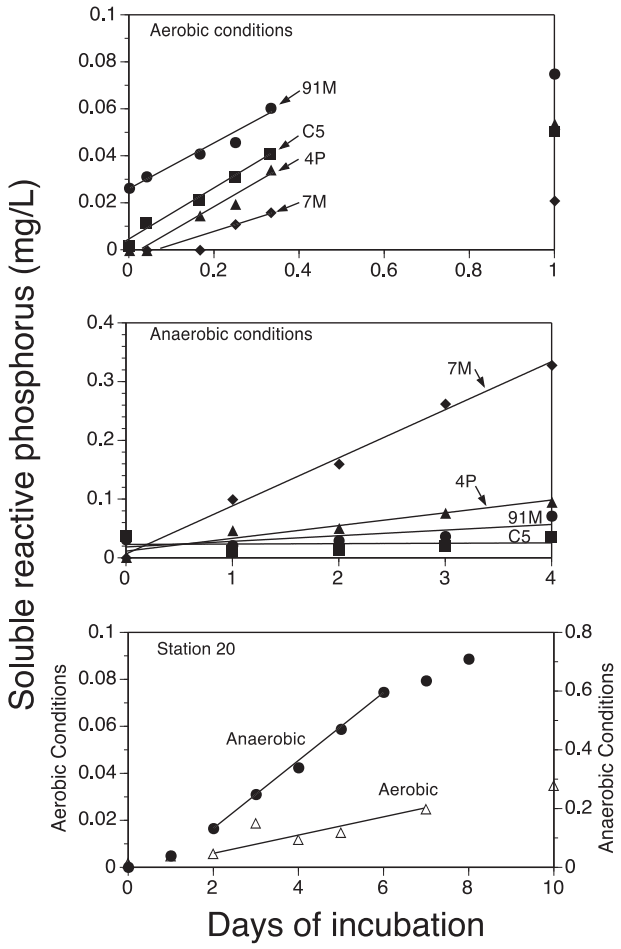

Fig. 2. Release of soluble reactive phosphorus (SRP) to the overlying water during incubation experiments. Top: aerobic incubation experiments from Stations 7M, 4P, 91M, and C5 conducted over 1 day. Center: anaerobic incubation experiments from Stations 7M, 4P, 91M, and C5 conducted over 4 days. Bottom: aerobic and anaerobic incubation experiments from Station 20 conducted over 10 days. Shown are regressions through linear portions of the data that were used to estimate the rate of phosphorus release from sediment.

incubations (unless otherwise stated, the uncertainties denote 1 standard deviation). Aerobic incubations are not subject to this change in chemistry that affects the P release rate. Although some incubations were relatively short (1 day), the data were very linear over the first 8 h so that data were used to calculate the rate of P release (Fig. 2). The average fluxes from the 1- and 10-day aerobic incubations were 1.30 ± 0.68 and 0.43 ± 0.27 mg P/m^2/day, respectively, and the difference between them was statistically significant ($p = 0.001$, 2-sample t-test); however, the measurements came from different locations in the lake. There is, as expected, a large difference between the aerobic and anaerobic incubations (average flux in aerobic incubations was 0.98 ± 0.78 mg P/m^2/day vs. 6.56 ± 6.05 mg P/m^2/day in anaerobic incubations; $p = 0.001$, 2-sample t-test). Fluxes under anaerobic conditions were 4–13 times greater than those under aerobic conditions when compared at the same locations. This is in agreement with other, recent findings. For example, North et al. (2015) reported fluxes under anaerobic conditions were about 9 times higher than those under aerobic conditions in Lake Diefenbaker.

In the bottom chambers the concentrations of SRP increased linearly with time over the sampling period and the dissolved oxygen concentrations decreased linearly with time over the first day or two and then decreased more slowly (Fig. 3), although none of the chambers went anaerobic during the sampling period. Measured P fluxes ranged from a low of 0.05 mg P/m^2/day at KI-SBI to a high of

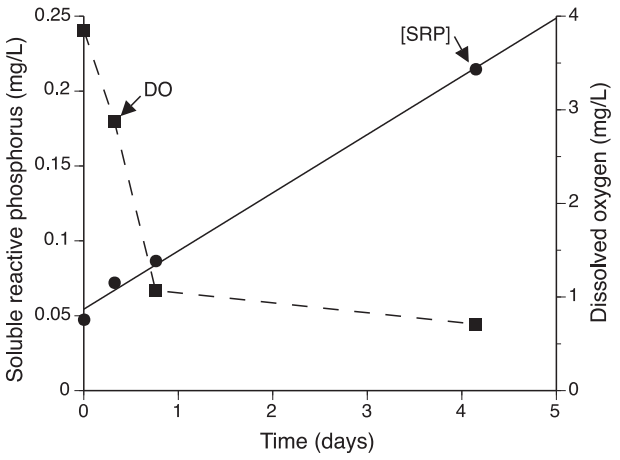

Fig. 3. Soluble reactive phosphorus (SRP) (circles, left axis) and dissolved oxygen (squares, right axis) concentrations versus time in a bottom chamber. *In situ* fluxes were calculated by volume correcting the SRP concentration versus time slopes to mass per time and dividing by the cross sectional area of the bottom chamber. Data from station WQ6.

2.97 mg P/m^2/day at WQ6. The fluxes do not appear to be related to TP concentrations in the sediment ($r = 0.181$, $p = 0.697$). However, the fluxes estimated by aerobic incubations and from bottom chambers appear to be well correlated with each other ($r = 0.988$, $p = 0.000$, although n, the number of comparisons, is only 6). For example, station WQ6 exhibited the highest aerobic incubation flux and the highest bottom chamber flux and station KI-SBI had the lowest aerobic incubation flux and the lowest bottom chamber flux. In addition, WQ6 exhibited the second highest sediment oxygen demand (SOD) (data not shown in Fig. 3) supporting the correlation between SOD and phosphate flux illustrated in Fig. 3.

Representative SRP microelectrode profiles for a sediment sample collected from location C5 are shown in Fig. 4. Under aerobic conditions, the phosphate concentrations were ~0 mg/L SRP in the overlying water and at the sediment surface, whereas under anaerobic conditions the SRP concentrations were 0.73 mg/L and 2.1 mg/L in the overlying water and at the sediment surface, respectively. These concentration profiles permit estimation of the concentration gradient in the diffusive boundary layer and calculation of the flux of SRP from the sediment into the overlying water. The fluxes were calculated from the concentrations in the overlying water and at the sediment–water interface assuming Fickian diffusion across the sediment–water interface according to Eqs. (7)–(9) as described in the Methods, and the results are given in Table 1. The calculated fluxes are in the range of those obtained using other techniques, although there are only 3 values for comparison.

A representative phosphate DET gel, from Station WQ2, is shown in Fig. 5. The hydrogel with colorimetrically developed color was scanned, calibrated, digitized, and artificially colorized and is shown in the left panel. It is apparent that the phosphate concentrations in the aerobic overlying water are lower than those in the anaerobic sediments. It is also apparent that the phosphate concentrations are highly variable within the sediments varying by as much as 12 mg/L over a distance of less than 1 cm. The sediment–water interface, which was not flat, is sketched in with a white dashed line to permit easier observation. Because of these variations in concentration and in the position of the sediment–water interface, 9 vertical sections were taken and converted to 1-dimensional profiles to permit determination of the concentration gradients (right panel). The dashed lines are linear fits to the topmost few mm of the concentration profiles, for clarity shown only for slices 1 and 3. The slopes of the lines represent the SRP concentration gradient used to calculate fluxes assuming Fickian diffusion across the sediment–water interface according to Eq. (2) and as described in the Methods, and the results are given in Table 1. Calculated fluxes ranged from a low of 0.60 mg P/m^2/day at Station BIM to a high of 8.26 mg P/m^2/day

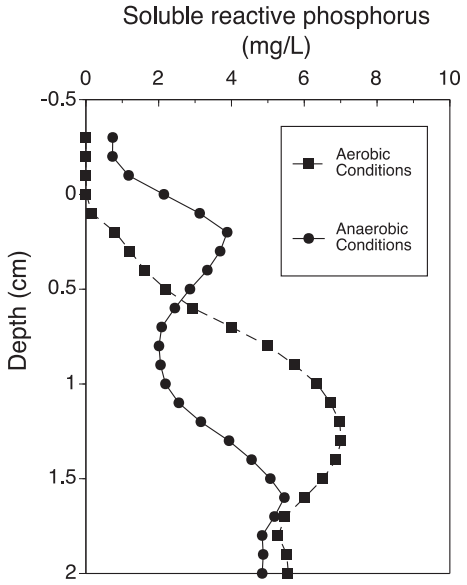

Fig. 4. Representative SRP concentration profiles collected from location C5 using the P-electrode for a sediment sample under both aerobic and anaerobic overlying water conditions.

at Station WQ6. There is no correlation between the fluxes calculated from aerobic incubations and from the DET gels ($r = 0.376$, $p = 0.284$), although both methods report their average highest fluxes at Station WQ6 and their average lowest fluxes at Station BIM. The DET gels may be better correlated with the anaerobic incubation fluxes ($r = 0.924$, $p = 0.250$, but n is only 3).

The calculated flux using the uppermost two expressed pore water concentrations at station 91M was 0.79 mg P/m^2/day (Fig. 6, left panel), within the range reported by the other methods (Table 1), although there is only 1 value for comparison.

The mass balance model is based on the concept that the diagenetic loss of organic *P* upon burial (Fig. 6, center panel) results in a release of dissolved phosphate that can either be buried or will diffuse back into the water column (Fig. 6, right panel). The flux of P from the sediment

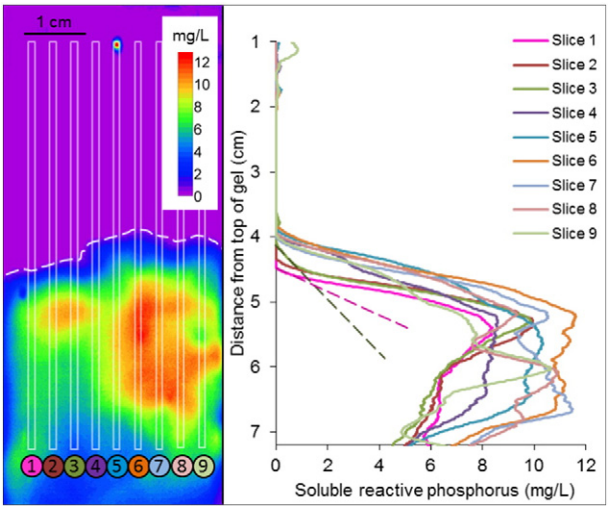

Fig. 5. Left panel: calibrated and colorized diffusive equilibrium in thin films (DET) gel illustrating the distribution of SRP near the sediment–water interface and location of the 9 rectangular slices of the image used to obtain concentration vs. depth profiles. Dashed line indicates sediment–water interface. Right panel: SRP concentration vs. depth profiles obtained for 9 slices of the same DET gel. Data from WQ2.

to the overlying water, $J_{p,s\text{-}w}$, is calculated from the difference between the depositional flux of organic *P* and the sum of the burial fluxes of organic *P* and dissolved phosphate. This method assumes that the precipitation of any P-bearing mineral phase in the surface sediment is matched by dissolution of the phase below such that there are no reactions that retain a portion of the released phosphate. As such, the calculated flux, 4.93 mg P/m^2/day at Station 91M, is in the range of both the anaerobic incubations and aerobic incubations (Table 1).

The sediment pore water chemistry and sediment solids fit the standard diagenetic model in which oxygen, nitrate and other electron acceptors are sequentially reduced and organic matter is oxidized liberating nutrients such as phosphate and ammonium to the pore water. These reactions have been simulated using the model of Dittrich et al. (2009), and the results are shown in Fig. 7. Aerobic respiration causes the rapid consumption of oxygen in the upper centimeter of the sediment column, and the model captures this rapid decrease in oxygen concentration although the model extends the zone of aerobic respiration to a depth of about 3 cm. Phosphate concentrations show some scatter, but the model fit describes well the general down-core decrease in concentrations. The diagenetic reactions oxidize organic carbon and the model approximates well the values of these data. pH is a very sensitive indicator of all the reactions occurring in the sediment, and the model describes well the surface decrease in pH from about 7.8 to 7.3. The P flux from the sediment calculated from the model is 2.38 mg P/m^2/day (Table 1), and it agrees reasonably well with the fluxes obtained from other methods, although this is the only station for which a comprehensive pore water and sediment solids data set was obtained permitting diagenetic modeling.

Analysis of multiple cores collected at the same sampling station (within a few meters apart) reveal up to 4-fold differences in calculated fluxes, indicating strong spatial variability of SRP gradients near sediment–water interface. For example, DET-calculated fluxes for duplicate cores from the station NBlw were 5.56 and 2.06 mg/m^2/day, and duplicate cores measured by aerobic incubations at station KI-SBI are 0.44 and 1.26 mg/m^2/day. Moreover, analyses of the standard deviation (SD) of (1) the average fluxes obtained by different methods for each station and (2) the average fluxes obtained from different stations using the same method revealed that there is no more variability between the stations (SD = 1.16 mg P/m^2/day) than there is between particular methods for each station (SD = 1.13 mg P/m^2/day). Due to the strong core to core variability of the flux, comparisons of average fluxes for particular stations and their relative locations in the western basin of Lake Erie are not possible. A comparison of all derived fluxes from all locations is given in Fig. 8. To prepare the summary in Fig. 8, all fluxes in Table 1 from any one method at any one location were averaged and their standard error calculated and those values are plotted adjacent to similarly calculated values for all methods. Immediately apparent from Fig. 8 is that in 10 of 11 cases the measured fluxes in anaerobic conditions were higher than those obtained under aerobic conditions. Because the western basin of Lake Erie is shallow and well mixed, anaerobic conditions are not expected to persist for periods of time longer than about 5 days (Bridgeman et al., 2006), thus anaerobic fluxes are not expected to contribute significantly to the total annual flux.

Among methods under aerobic conditions the DET stands out as yielding the highest fluxes, although at many locations the DET generated fluxes are comparable to those from other methods. Fluxes determined from the bottom chambers are comparable to those determined in the aerobic incubations, although they are slightly lower except in one case. Fluxes under aerobic conditions at the eastern and northern sites are lower than those at the southwestern sites near the Maumee River discharge.

Discussion

We have used a variety of methods to estimate the flux of P from sediment to the water column, and each method has it uncertainties.

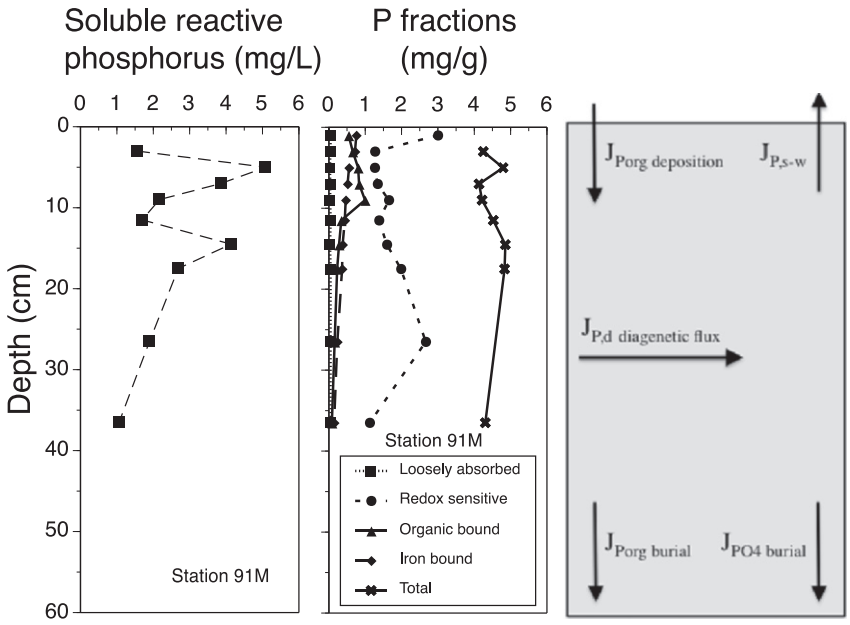

Fig. 6. Left panel: Expressed pore water soluble reactive phosphorus (SRP) concentration profile used to calculate the SRP flux assuming Fickian diffusion across the sediment–water interface. Center panel: phosphorus fractions in sediment solids. The organic bound fraction is used in the calculation of the phosphorus flux using the mass balance model (Eq. 10). Right panel: schematic illustrating the mass balance model.

Fluxes obtained directly, such as by incubation or with the bottom chambers which were not opaque, probably underestimate the diffusive flux of phosphate because of algal and/or microbial uptake during incubations. Additionally, P released into the water column in core tubes or plastic bottom chambers may be subject to significant sorption; for example, Holdren and Armstrong (1980) measured a 61% loss of P in just 1 day, and a 90% loss in a 4-day experiment with acrylic plastic. On the other hand, fluxes obtained by Fickian diffusion calculations, such as the DET, expressed pore water, and the P-electrode, are subject to uncertainty due to the assumption that transport is controlled only by Fickian diffusion between the pore water and the overlying water, which may not be true for such a complex and dynamic system like the lake bottom, particularly in the presence of wave action in shallow basins. Concentration gradient-based flux calculations are also influenced by the choice of the depth interval used and limited by the spatial resolution of the measurement method. For example, pore water expressed at 0.5 or 1 cm intervals may not adequately describe the gradients at the sediment–water interface or in the diffusive boundary layer, which is typically less than 1 mm thick (Wang et al., 1982). While each one of the methods has its limitations and difficulties and the "true" value of the flux is not known, by combining together the values from different methods, we are able to effectively bracket the range of the most probable SRP flux. However, if a person wanted to use only one method to obtain an estimate of the flux, our recommendation would be core incubations because (1) they are a direct measurement (not calculated) of the SRP accumulation in the water column, (2) they represent the average from the entire surface of the core which partially eliminates the effect of the strong spatial variability of exchangeable phosphate in sediment, and (3) they are easier to measure than bottom chambers but offer comparable results.

From the data in Table 1, the fluxes from any one method at each station (replicate measurements) were averaged and then the fluxes from all methods at each station were equally weighted to obtain an average flux at that location. These station averages were then averaged across all stations to obtain an estimate of the summertime average basin-wide aerobic and anaerobic fluxes. The average summertime aerobic P flux was 1.35 mg/m^2/day, with a 95% confidence interval of 0.95 to 1.79 mg/m^2/day, and the average summertime anaerobic P flux was 6.01, with a 95% confidence interval of 1.84 to 8.18 mg/m^2/day. On average, fluxes under anaerobic conditions are 4 to 13 times larger than those under aerobic conditions, in agreement with the ~9 times higher values reported by North et al. (2015) for Lake Diefenbaker. Suppressed P accumulation in the overlying water column under aerobic conditions is consistent with the classic Mortimer (1941) model of coupled Fe-P chemistry. Under this scenario, Fe is in an oxidized state as a ferric oxyhydroxide (FeOOH) in the aerobic sediment microzone (i.e., the thin aerobic surface sediment layer often less than 1 mm in thickness) and strongly adsorbs P, resulting in very limited P diffusion into the overlying water column. The greater flux under anaerobic conditions is probably related to microbial reduction of Fe under anaerobic conditions, desorption of P into porewater, and subsequent diffusion into the overlying water column. Aerobic conditions at the sediment–water interface probably dominate redox chemistry in the western basin because of the shallow, mixed environment, but this process may still have some importance there since the shallow water of the western basin can occasionally stratify for time periods of up to 5 days and the bottom waters can go anaerobic (Bridgeman et al., 2006). Although P release is much lower under aerobic conditions, sediments still appeared to represent a potentially important direct source of P for algal assimilation.

Because iron oxyhydroxides are one of the major constituents in sediment responsible for SRP binding, it was hypothesized that DET images of dissolved iron (II) would be directly correlated to SRP distribution, due to the fact that reduction of strongly sorptive iron precipitates should release bound P. However, no such correlation was observed (images not shown). Generally, the cores with high concentration of iron also have a significant amount of SRP, but there are also cores with high iron concentrations and low SRP concentrations (e.g., 91M) and cores with low iron concentrations and high SRP concentrations (e.g., NBlw). More detailed analysis of the regions of high and low analyte concentrations failed to show either a direct or an inverse correlation between iron (II) and SRP. We interpret this to mean that reduction of iron oxyhydroxides to iron (II) and simultaneous release of the bound fraction of SRP is not the main process controlling P release to western Lake Erie as measured by any of the methods under aerobic conditions. This is consistent with the conclusions of Moore

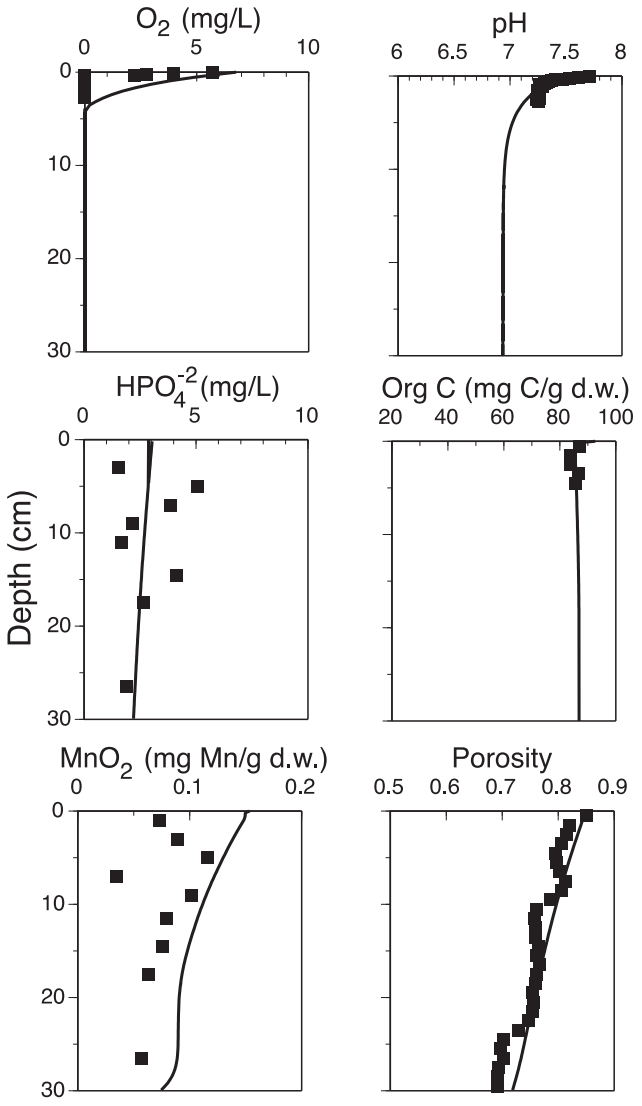

Fig. 7. Pore water and sediment concentrations and model fits from Station 91M using the biogeochemical model of Dittrich et al. (2009). SRP fluxes were calculated assuming Fickian diffusion across the sediment–water interface.

et al. (1998) who suggested that it is not the diffusion from reduced sediments but rather precipitation and sorption in the surficial oxidized sediment layer that is responsible for P retention or release.

Comparison of sediment P concentrations and aerobic SRP fluxes suggests that there is no statistically significant correlation between the overall SRP flux and total sediment P ($r = -0.008$, $p = 0.976$). This is consistent with the findings of Jensen et al. (1992) who found no correlation between the water total P and the sediment P in Danish lakes. However, they were able to correlate water total P with sediment Fe:P ratio, which provides an estimate of the sediment's phosphate sorption capacity. Also, it must be noted that due to the large standard deviation the mean aerobic fluxes at a particular station are not statistically different from each other at the 0.05 significance level (ANOVA, Tukey test).

Dreissenid populations (zebra and quagga mussels) may be a factor in the P release rates and station-to-station variability. For example, Dittrich et al. (2013) hypothesized that dreissenid colonization of Cook's Bay in Lake Simcoe decreased P retention in the sediment. Gudimov et al. (2015) modeled the P mass balance in Lake Simcoe and similarly concluded that the colonization by dreissenids and the recent proliferation of macrophytes appear to have decreased P retention. At our sites, Stations 1, 19, and 20 did not have visible mussels, but Stations 25 and 27 did have mussels and the measured fluxes from the sites with mussels were greater than those at the other sites. This is true under both aerobic and anaerobic conditions. Dreissenid mussels are known to release phosphate in addition to sediment diffusive flux (James et al., 2001), so both lab incubations and bottom chamber results are affected by their inputs. Anaerobic incubations may have inadvertently killed any mussels, resulting in additional P flux. Under aerobic conditions, mussels can actively recycle P as soluble P and also release it during periods of starvation and emaciation. The effect of presence or absence of dressenids between cores 25 and 27, and cores 1, 19 and 20, is difficult to measure due to different sediment compositions at these locations. Consequently, it is not possible to directly determine the true diffusive P flux in the western basin due to dreissenid mussel influences. The burrowing behavior of mayfly nymphs (*Hexagenia* spp.) can also increase P concentrations in overlying water at high densities (Chaffin and Kane, 2010), but we did not observe nymphs in cores and divers could not determine presence of nymphs in bottom chambers. The presence of worm burrows (most likely oligochaetes) was also observed in some of the cores during DET analysis; however, they did not correlate with increased P fluxes. There is no clear evidence for increased SRP flux in the presence of macrobenthos measured in this study, except possibly at stations 25 and 27. Therefore, we assume that our measurements of SRP flux do not include the P recycled by macrobenthos. However, the effects of bioturbation, particularly by the abundant dreissenids, have to be considered in large scale, basin-wide models. More details about the effect of dreissenids on SRP in Lake Erie can be found in Karatayev et al. (2015) and Zhang et al. (2011).

It is possible to use this spatially dispersed sampling to extrapolate these results to obtain an estimate of the overall basin-wide diffusive flux of P from sediments. Because the western basin of Lake Erie is likely to be well mixed and aerobic throughout the water column most of the time (MacIsaac et al., 1992; MacIsaac et al., 1999; Zhang et al., 2011), we based this calculation on the fluxes measured under aerobic conditions only. It is possible that that this approach may underestimate the internal SRP flux by neglecting the potential effect of anoxia and polymixis. While stratification and consequent anoxia in the bottom waters are not typical of the western basin of Lake Erie (MacIsaac et al., 1992; MacIsaac et al., 1999; Zhang et al., 2011), the lake can occasionally stratify for periods of 4 or 5 days, leading to anoxia (Bridgeman et al., 2006).

The P fluxes reported in Table 1 are based on field and laboratory measurements made during the warmest time of the year, so it is likely that they overestimate the annual fluxes. High temperatures increase rates of P regeneration in sediments and increase the diffusion coefficients. During months with high primary production, increased dead algal matter on the sediment surface may deplete dissolved oxygen and decrease the thickness of the oxidized layer at the sediment–water interface and thereby increase the rate of release of P from redox-sensitive iron oxides. Dead algal cells have been also shown to rapidly release SRP, for example, Golterman (1975) observed that up to 80% of P was released as phosphate within 3 days after induced autolysis. Thus, algal matter deposited on the sediment surface may become an additional source of SRP, aside from phosphorus diffusing from the sediment.

While North et al. (2015) reported that winter values of internal P flux were about 35% higher than summer values, the majority of the studies suggest otherwise. For example, the compilation of 29 P release rates measurements conducted at different temperatures and compiled by Holdren and Armstrong (1980) shows that the P release rates from sediments at 7 °C are very low, often close to zero, and sometimes even negative. A study of 16 Danish lakes conducted by Søndergaard et al. (1999) suggests even stronger negative P release in sediments during winter months, which the author attributes to decreased temperature and biological activity. Because of the high lake-to-lake variability of the seasonal changes in SRP release from sediments, it is not possible to precisely predict the winter fluxes in western Lake Erie based on the summer flux measurements. However, with the majority of the

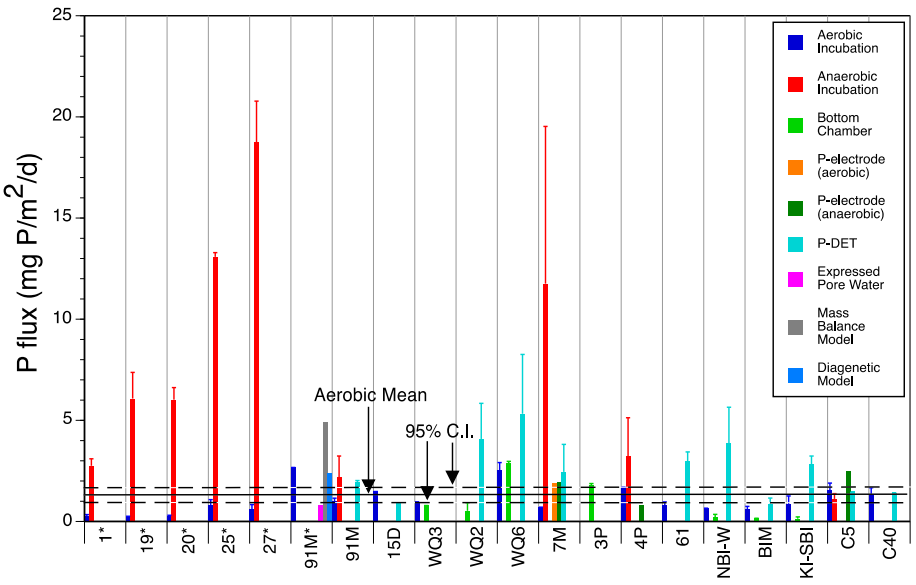

Fig. 8. Summary of summertime P fluxes comparing all methods from all stations. * Data from 2013; all other data from 2014. Standard error shown for those methods for which replicate fluxes were determined.

reported studies on other lakes concluding lower diffusive fluxes in winter, we can adjust our measured summertime fluxes to account for the lower temperatures during the rest of the year to obtain an annual estimate of the internal flux. Here we assume that the flux is directly proportional to the diffusion coefficient as described in Eq. (2) and that the temperature dependency of the diffusion coefficient is well described by either the Stokes-Einstein relation as shown in Li and Gregory (1974) where the diffusion coefficient at 25 °C is 2.19 times the value at 0 °C or by DiToro (2001) and Testa et al. (2013) where the diffusion coefficient is temperature corrected by a factor of $1.08^{(T-20)}$ where T is the temperature (°C). Assuming an average annual bottom water temperature of 10 °C, then using the Li and Gregory (1974) correction the annual aerobic P flux would be expected to be about 0.67 times our measured summertime values. This yields a mean annual aerobic flux of 0.91 mg P/m^2/day with a 95% confidence interval of 0.64 to 1.21 mg/m^2/day. The western basin is about 12.8% of the total 25,657 km^2 area of Lake Erie, or 3284 km^2. Using the average annual aerobic flux yields a western basin-wide total 808 Mg P/year with a 95% confidence interval of between 768 and 1422 Mg P/year as the diffusive flux from sediments. Using the DiToro (2001) and the Testa et al. (2013) temperature correction factor, the annual aerobic P flux would be expected to be about 0.32 times our measured summertime values. This yields a mean annual aerobic flux of 0.43 mg P/m^2/day with a 95% confidence interval of 0.30 to 0.56 mg/m^2/day for a western basin-wide total of 378 Mg P/year with a 95% confidence interval of between 359 and 665 Mg P/year as the diffusive flux from sediments.

These basin-wide estimates of the annual diffusive P flux are in excellent agreement with the 484-Mg P/year flux derived using the western Lake Erie Ecosystem Model (WLEEM) (E. Verhamme, LimnoTech, personal communication, January 22, 2016). The WLEEM model is a deterministic, fine-scale, three-dimensional, linked hydrodynamic-sediment transport-eutrophication model designed to estimate internal and external nutrient dynamics within western Lake Erie (Verhamme et al., 2016). The sediment diagenesis sub-model is based on DiToro (2001) and Testa et al. (2013) and accounts for spatial differences of sediment conditions, fluxes of organic *P* to the sediment, and temperature changes over the season to correct diffusion rates. For 2014, the average basin-wide diffusive fluxes of P from the sediments ranged from 0.06 mg/m^2/day during winter months to over 1.25 mg/m^2/day in summer months, with an annual average flux of 0.44 mg/m^2/day.

Our estimates of the mean annual diffusive P flux ranges from 3% to 7%, depending on the temperature correction, of the 11,000-Mg P/year IJC target load for P delivery to Lake Erie from external sources, significantly less than the 45–89% estimate for Lake Simcoe (Nürnberg et al., 2013). Recently, the Annex 4 committee of the 2012 GLWQA recommended a new target TP load of 6000 Mg P/year, and our internal P flux would be 6–13%, depending on the temperature correction, of the new external target load.

It is also possible to estimate the contribution of the internal flux to the total SRP concentration in the water column as the flux divided by the water depth times the residence time of the water. The residence time of water in the western basin may be estimated from the volume of water in the basin divided by the rate of water flow into the basin. The western basin is about 3284 km^2 in area, and it averages 7.3 m water depth for a volume of 2.40×10^{10} m^3. The water inflow to the western basin can be approximated as the sum of the Detroit River discharge (5324 m^3/s) and the Maumee River discharge (150 m^3/s) and is about 4.73×10^8 m^3/day. This gives an average residence time of 50.7 days. For the mean annual aerobic flux between 0.43 and 0.91 mg P/m^2/day, depending on the temperature correction, a 7.3-m deep water column and assuming uniform vertical and spatial mixing with an average water residence time of 50.7 days, it can be calculated that the sediment contributes between 3.0 and 6.3 μg/L of dissolved P to the water column. This contribution represents 20–42% of the IJC Target Concentration of 15 μg P/L for the western basin.

The implication of these calculations for Lake Erie is that this internal diffusive recycling of P, essentially constituting a "background" P input, is unlikely to trigger cyanobacterial blooms by itself, but it is sufficiently large to cause blooms when combined with external loads. This background flux may be also responsible for delayed response of the lake to any decrease in the external loading. Furthermore, the seasonally dependent sediment storage and subsequent internal release of phosphate may play an important role in the lag time between spring time P loads and summer/fall time blooms.

Acknowledgments

This work was supported by an EPA Great Lakes Restoration Initiative project GL-00E01284 to the Ohio Lake Erie Commission. Portions of the work were also supported by Ohio Sea Grant project RES123861, the Lake Erie Protection Fund project number SG 445-

2013, and the U.S. Army Engineer District–Buffalo. The authors acknowledge Kevin Hart, Matt Thomas, Gregory Kennedy, Glen Black, and Tyler Steube for assisting with chamber deployment, sampling, and retrieval. C. Behnke, J. DePinto, and E. Verhamme of LimnoTech (Ann Arbor, MI) are thanked for organizing and executing a portion of the sediment core collection for laboratory incubation and for providing data and comments to improve the manuscript. The authors would also like to thank the EPA for providing ship time and the crew of the R/V Lake Guardian. The paper benefited from reviews by J. DePinto, J. Larson, and two anonymous reviewers. This is publication 2016 of the U.S. Geological Survey Great Lakes Science Center. Any use of trade, product, or firm names is for descriptive purposes only and does not imply endorsement by the U.S. Government.

References

American Public Health Association, 1989. American Waterworks Association, and Water Pollution Control Federation. Standard Methods for the Examination of Water and Wastewater, 17th ed. American Public Health Association, Washington, D.C.

Baker, D.B., Confessor, R., Ewing, D.E., Johnson, L.T., Kramer, J.W., Merryfield, B.J., 2014. Phosphorus loading to Lake Erie from the Maumee, Sandusky and Cuyahoga rivers: the importance of bioavailability. J. Great Lakes Res. 40, 502–517.

Bertram, P.E., 1993. Total phosphorus and dissolved oxygen trends in the central basin of Lake Erie, 1970–1991. J. Great Lakes Res. 19, 224–236.

Boström, B., Andersen, J.M., Fleischer, S., Jansson, M., 1998. Exchange of phosphorus across the sediment–water interface. Hydrobiologia 170, 229–244.

Boudreau, B.B., 1996. The diffusive tortuosity of fine-grained unlithified sediments. Geochem. Cosmochim. Acta 60 (16), 3139–3142.

Bridgeman, T.B., Schloesser, D.W., Krause, A.E., 2006. Recruitment of *Hexagenia* mayfly nymphs in western Lake Erie linked to environmental variability. Ecol. Appl. 16, 601–611.

Canavan, R., Slomp, C., Jourabchi, P., Van Cappellen, P., Laverman, A., van den Berg, G., 2006. Organic matter mineralization in sediment of a coastal freshwater lake and response to salinization. Geochim. Cosmochim. Acta 70, 2836–2855.

Chaffin, J.D., Kane, D.D., 2010. Burrowing mayfly (Ephemeroptera: Ephemeridae: *Hexagenia* spp.) bioturbation and bioirrigation: a source of internal phosphorus loading in Lake Erie. J. Great Lakes Res. 36, 57–63.

Chaffin, J.D., Bridgeman, T.B., Bade, D.L., 2013. Nitrogen constrains the growth of late summer cyanobacterial blooms in Lake Erie. Adv. Microbiol. 3, 16–26.

Charlton, M.N., 1980. Hypolimnion oxygen consumption in lakes: discussion of productivity and morphometry effects. Can. J. Fish. Aquat. Sci. 37, 1531–1539.

Conroy, J.D., Edwards, W.J., Pontius, R.A., Kane, D.D., Zhang, H., Shea, J.F., 2005b. Soluble nitrogen and phosphorus excretion of exotic freshwater mussels (*Dreissena* spp.): potential impacts for nutrient remineralisation in western Lake Erie. Freshw. Biol. 50, 1146–1162.

Conroy, J.D., Kane, D.D., Dolan, D.M., Edwards, W.J., Charlton, M.N., Culver, D.A., 2005a. Temporal trends in Lake Erie plankton biomass: roles of external phosphorus loading and dreissenid mussels. J. Great Lakes Res. 31 (Suppl. 2), 89–110.

Davison, W., Fones, G., Harper, M., Teasdale, P., Zhang, H., 2000. Dialysis, DET and DGT: in situ diffusional techniques for studying water, sediments and soils. In: Buffle, J., Horvai, G. (Eds.), In Situ Monitoring of Aquatic Systems –chemical analysis and speciation. IUPAC, Wiley, Chichester, pp. 495–569.

DePinto, J.V., Young, T.C., McIlroy, L.M., 1986. Impact of phosphorus control measures on water quality of the Great Lakes. Environ. Sci. Technol. 20 (8), 752–759.

Di Toro, D.M., Connolly, J.P., 1980. Mathematical models of water quality in large lakes. Part 2: Lake Erie. U.S.EPA Report #EPA-600/3–80-065.

Ding, X., Behbahani, M., Gruden, C., Seo, Y., 2015. Characterization and evaluation of phosphate microsensors to monitor internal phosphorus loading in Lake Erie sediments. J. Environ. Manag. 160, 193–200.

DiToro, D.M., 2001. Sediment Flux Modeling. Wiley $_amp_$amp; Sons, Inc.

Dittrich, M., Chesnyuk, A., Gudimov, A., McCulloch, J., Quaizi, S., Young, J., Winter, J., Stainsby, E., Arhonditsis, G., 2013. Phosphorus retention in a mesotrophic lake under transient loading conditions: insights from a sediment phosphorus binding form study. Water Res. 47 (3), 1433–1447.

Dittrich, M., Wehrli, B., Reichert, P., 2009. Lake sediments during the transient eutrophication period: reactive-transport model and identifiability study. Ecol. Model. 220, 2751–2769.

Elsbury, K.E., Paytan, A., Ostrom, N.E., Kendall, C., Young, M.B., McLaughlin, K., Rollog, M.E., Watson, S., 2009. Using oxygen isotopes of phosphate to trace phosphorus sources an cycling in Lake Erie. Environ. Sci. Technol. 43, 3108–3114.

Golterman, H.L., 1975. Physiological Limnology. Elsevier Science Publishing Company, Amsterdam (489 pp.).

Gudimov, A., Kim, D.-K., Young, J.D., Palmer, M.E., Dittrich, M., Winter, J.G., Stainsby, E., Arhonditsis, G.B., 2015. Examination of the role of dreissenids and macrophytes in the phosphorus dynamics of Lake Simcoe, Ontario, Canada. Ecol. Inform. 26, 36–53.

Gunnars, A., Blomqvist, S., 1997. Phosphate exchange across the sediment–water interface when shifting from anoxic to oxic conditions—an experimental comparison of freshwater and brackish-marine systems. Biogeochemistry 37, 203–226.

Hoffman, A.R., Armstrong, D.E., Lathrop, R.C., 2013. Influence of phosphorus scavenging by iron in contrasting dimictic lakes. Can. J. Fish. Aquat. Sci. 70, 941–952.

Holdren, G.C., Armstrong, D.E., 1980. Factors affecting phosphorus release from intact lake sediment cores. Environ. Sci. Technol. 14, 79–87.

James, W.F., Barko, J.F., Eakin, H.L., 2001. Phosphorus recycling by zebra mussels in relation to density and food resource availability. Hydrobiologia 455 (1–3), 55–60.

James, W.F., 2012. Estimation of Internal Phosphorus Loading Contributions to the Lake of the Woods. Minnesota, ERDC Report (42 pp.).

Jensen, H.S., Kristensen, P., Jeppesen, E., Skyttthe, A., 1992. Iron:phosphorus ratio in surface sediment as an indicator or phosphate release from aerobic sediments in shallow lakes. Hydrobiologia 235 (236), 731–743.

Jézéquel, D., Brayner, R., Metzger, E., Viollier, E., Prévot, F., Fiévet, F., 2007. Two-dimensional determination of dissolved iron and sulfur species in marine sediment pore-waters by thin-film based imaging. Thau lagoon (France). Estuar. Coast. Shelf Sci. 72, 420–431.

Korostynska, O., Mason, A., Al-Shamma'a, A., 2012. Monitoring of nitrates and phosphates in wastewater: current technologies and further challenges. Int. J. Smart Sens. Intell. Syst. 5 (1), 149–176.

Karatayev, A.Y., Burlakova, L.E., Padilla, D.K., 2015. Zebra versus quaga mussels: a review of their spread, population dynamics, and ecosystem impacts. Hydrobiologia 746, 97–112.

Krom, M.D., Berner, R.A., 1980. Adsorption of phosphate in anoxic marine sediments. Limnol. Oceanogr. 25 (5), 797–806.

Lee, W.H., Bishop, P.L., 2009. In situ microscale analyses of activated sludge flocs in the enhanced biological phosphate removal process by the use of microelectrodes and fluorescent in situ hybridization. J. Environ. Eng. 136 (6), 561–567.

Lee, W.H., Seo, Y., Bishop, P.L., 2009. Characterization and evaluation of the cobalt-based phosphate microelectrode for use in-vivo environmental analysis. Sensors Actuators B 137, 121–128 (PMID: 20161285).

Lewandowski, Z., Beyenal, H., 2014. Fundamentals of Biofilm Research. Second Edition. CRC Press, Taylor and Francis Group.

Li, Y., Gregory, S., 1974. Diffusion of ions in sea water and in deep-sea sediments. Geochim. Cosmochim. Acta 38, 703–714.

Loh, P.S., Molot, L.A., Nürnberg, G.K., Watson, S.B., Ginn, B., 2013. Evaluating relationships between sediment chemistry and anoxic phosphorus and iron release across three different water bodies. Inland Waters 3, 105–118.

MacIsaac, H.J., Johannsson, O.E., Ye, J., Sprules, W.G., Leach, J.H., McCorquodale, J.A., Grigorovich, I.A., 1999. Filtering impacts of an introduced bivalve (*Dreissena polymorpha*) in a shallow lake: application of a hydrodynamic model. Ecosystems 2, 338–350.

MacIsaac, H.J., Sprules, W.G., Johannsson, O.E., Leach, J.H., 1992. Filtering impacts of larval and sessile zebra mussels (*Dreissena polymorpha*) in western Lake Erie. Oecologia 92, 30–39.

Makarewicz, J.C., 1993. Phytoplankton as indicators of environmental health. Verh. Internat. Verein. Limnol. 25, 363–365.

Matisoff, G., Ciborowski, J., 2005. Lake Erie trophic status collaborative study. J. Great Lakes Res. 31 (Suppl. 2), 1–10.

Michalak, A.M., Anderson, E.J., Beletsky, D., Boland, S., Bosch, N.S., Bridgeman, T.B., Chaffin, J.D., Kyunghwa, H.C., Confesor, R., Daloglu, I., DePinto, J., Evans, M.-E., Fahnenstiel, G.L., He, L., Ho, J.C., Jenkins, L., Johengen, T., Kuo, K.C., LaPorte, E., Liu, X., McWilliams, M., Moore, M.R., Posselt, D.J., Richards, R.P., Scavia, E., Steiner, A.L., Verhamme, E., Wright, D.M., Zagorski, M.A., 2013. Record-setting algal bloom in Lake Erie caused by agricultural and meteorological trends consistent with expected future conditions. Proc. Natl. Acad. Sci. 110 (16), 6448–6452 (April 16, 2013).

Moore, P.A., Reddy, K.R., Fisher, M.M., 1998. Phosphorus flux between sediment and overlying water in Lake Okeechobee, Florida: spatial and temporal variations. J. Environ. Qual. 27, 1428–1439.

Mortimer, C.H., 1941. The exchange of dissolved substances between mud and water. J. Ecol. 29, 280–329.

Noffke, A., Hensen, C., Sommer, S., Scholz, F., Bohlen, L., Mosch, T., Graco, M., Wallmann, K., 2012. Benthic iron and phosphorus fluxes across the Peruvian oxygen minimum zone. Limnol. Oceanogr. 57, 851–867.

North, R.L., Johansson, J., Vandergucht, D., Doig, L.E., Liber, K., Lindenschmidt, K.-E., Baulch, H., Hudson, J.J., 2015. Evidence for internal phosphorus loading in a large prairie reservoir (Lake Diefenbaker, Saskatchewan). J. Great Lakes Res. 41 (Suppl. 2), 91–99. http://dx.doi.org/10.1016/j.jglr.2015.07.003.

Nürnberg, G.K., LaZerte, B.D., Loh, P.S., Molot, L.A., 2013. Quantification of internal phosphorus load in large, partially polymictic and mesotrophic Lake Simcoe, Ontario. J. Great Lakes Res. 39, 271–279.

Obenour, D.R., Gronewold, A.D., Stow, C.A., Scavia, D., 2014. Using a Bayesian hierarchical model to improve Lake Erie cyanobacteria bloom forecasts. Water Resour. Res. 50, 7847–7860.

Ohio Environmental Protection Agency (Ohio EPA), 2010. Ohio Lake Erie Phosphorus Task Force Final Report. (Columbus, OH., Available at) http://epa.ohio.gov/portals/35/lakeerie/ptaskforce/Task_Force_Final_Report_April_2010.pdf. (Last accessed July 15, 2015).

Orihel, D.M., Schindler, D.W., Ballard, N.C., Graham, M.D., O'Connell, D.W., Wilson, L.R., Vinebrooke, R.D., 2015. The "nutrient pump:" iron-poor sediments fuel low nitrogen-phosphorus ratios and cyanobacterial blooms in polymictic lakes. Limnol. Oceanogr. http://dx.doi.org/10.1002/lno.10076.

Petzold, L., 1983. A description of DASSL: a differential/algebraic system solver. In: Stepleman, R.E. (Ed.), Scientific Computing. IMACS/North-Holland, Amsterdam, pp. 65–68.

Reichert, P., 1994. AQUASIM—a tool for simulation and data analysis of aquatic systems. Water Sci. Technol. 30, 21–30.

Reynolds, C.S., 2006. Ecology of Phytoplankton. Cambridge University Press.

Rockwell, D.C., Warren, G.J., 2003. Lake Erie report for the Great Lakes National Program Office's indicators monitoring program 1983–2002. 46th Annual Conf., Internat. Assoc. Great Lakes Res. Abstract, p. 70.

Schelske, C.L., Stoermer, E.F., 1971. Eutrophication, silica depletion and predicted changes in algal quality in Lake Michigan. Science 173, 423–424.
Schumacher, B.A., 2002. Methods for the determination of total organic carbon (TOC) in soils and sediments. U.S. EPA NCEA-C-1282, EMASC-001 23pp.
Søndergaard, M., Jensen, J.P., Jeppesen, E., 1999. Internal phosphorus loading in shallow Danish lakes. Hydrobiologia 408 (409), 145–152.
Søndergaard, M., Jensen, J.P., Jeppesen, E., 2003. Role of sediment and internal loading of phosphorus in shallow lakes. Hydrobiologia 506-509, 135–145.
Strickland, J.D.H., Parsons, T.R., 1972. A Practical Handbook of Seawater Analysis, Bulletin 167. second ed. Fisheries Research Board of Canada, Ottawa.
Stumpf, R.P., Wynne, T.T., Baker, D.B., Fahnenstiel, G.L., 2012. Interannual variability of cyanobacterial blooms in Lake Erie. PLoS One 7 (8), e42444. http://dx.doi.org/10.1371/journal.pone.0042444.
Tenberg, A., Stahl, H., Gust, G., Mueller, V., Arning, U., Andersson, H., Hall, P.O.J., 2004. Intercalibration of benthic flux chambers I. Accuracy of flux measurements and influence of chamber hydrodynamics. Prog. Oceanogr. 60, 1–28.
Testa, J.M., Damien, B.C., DiToro, D.M., Boyton, W.R., Cornwell, J.C., Kemp, W.M., 2013. Sediment flux modeling: simulating nitrogen, phosphorus, and silica cycles. Estuar. Coast. Shelf Sci. 131, 252–263.
Verhamme, E.M., Redder, T.M., Schlea, D., Grush, J., Bratton, J.F., DePinto, J.V., 2016. Development of the western Lake Erie Ecosystem Model (WLEEM): application to connect phosphorus loads to cyanobacteria biomass. J. Great Lakes Res. (In review to Annex 4 Special Issue).
Vollenweider, R.A., 1976. Advances in defining critical loading levels for phosphorus in lake eutrophication. Mem. Ist. Ital. Idrobiol. 33, 53–83.
Wang, J., Zhao, L., Wei, H., 1982. Variable diffusion boundary layer and diffusion flux at sediment–water interface in response to dynamic forcing over an intertidal mudflat. Chin. Sci. Bull. 57, 1568–1577.
Wang, Y., Van Cappellen, P., 1996. A multicomponent reactive transport model of early diagenesis: application to redox cycling in coastal marine sediments. Geochim. Cosmochim. Acta 60, 2993–3014.
Xiao, D., Yuan, H.-Y., Li, J., Yu, R.-Q., 1995. Surface-modified cobalt-based sensor as a phosphate-sensitive electrode. Anal. Chem. 67 (2), 288–291.
Zhang, H., Culver, D.A., Boegman, L., 2011. Dreissenids in Lake Erie: an algal filter or a fertilizer? Aquat. Invasions 6 (2), 175–194.